Numerical study of interaction between Darrieus-Landau instability and spatially periodic shear flow

Damir Valiev,[1] Andrea Gruber,[2] Chung K. Law,[3] Jacqueline H. Chen[4]
[1]Umeå University, Umeå, Sweden, [2]SINTEF Energy Research, Trondheim, Norway,
[3]Princeton University, Princeton, USA, [4]Sandia National Laboratories, Livermore, CA, USA

1 Motivation and Objectives

It was recently shown that Darrieus-Landau (DL) instability has a role in boundary layer flashback of premixed turbulent flames [1], actively contributing to flame acceleration through flame corrugation that, in turn, results in the creation of near-wall regions of flow reversal ahead of the flame sheet. The flame in the boundary layer behaves in a laminar fashion modulated by weak, highly anisotropic velocity fluctuations. It is seen that the flame acquires a corrugated shape with the characteristic time and length scales that can be correlated with the structures in the boundary layer. A snapshot of the typical flame shape obtained in the direct numerical simulation (DNS) of boundary layer flashback is shown on Fig. 1. The oncoming prolongated velocity streaks with alternating regions of relatively high and low velocities interact with the initially planar flame. The observed flame shape evolution suggests that the streaky structure of the flow triggers the corresponding unstable wavelength of DL instability, resulting in the flame acceleration and subsequent upstream propagation of a corrugated flame.

Recent experimental investigations have confirmed the existence of the above mentioned flow reversal regions in both swirling and non-swirling configurations [2, 3, 4], with flame propagation upstream with velocities approximately two times larger than the laminar burning velocity.

In Ref. [5] it was found that a planar that is subjected to oncoming periodic shear flow can propagate with increased velocities in the absence of thermal expansion. Several previous studies focused on the interaction of weak, homogeneous isotropic turbulence and DL instability. In Refs. [6, 7] it was found that the effect of DL instability may be dominant when the turbulence intensity is low. However, there still remain many open questions regarding the interaction of anisotropic velocity fluctuations and flames with realistic thermal expansion.

We perform a detailed investigation of the role of DL instability on the propagation regime of laminar flame front subjected to external forcing by a spatially periodic shear flow that resembles the turbulent boundary layer's streaky pattern. The present study is focused on identifying conditions for which either intrinsic flame spatial scales or streaky structure spatial scales would be dominant in the process. The parametric study is focused on the variation of flame configuration and propagation speed dependent upon the amplitude and spatial scale of the oncoming periodic shear flow. It is found that in two-dimensional simulations the flame shape may be dominated either by the oncoming shear flow or by the intrinsic flame DL instability. It is demonstrated that the shear-flow induced flame shape may be unstable and undergo changes during the simulation run, being replaced by DL

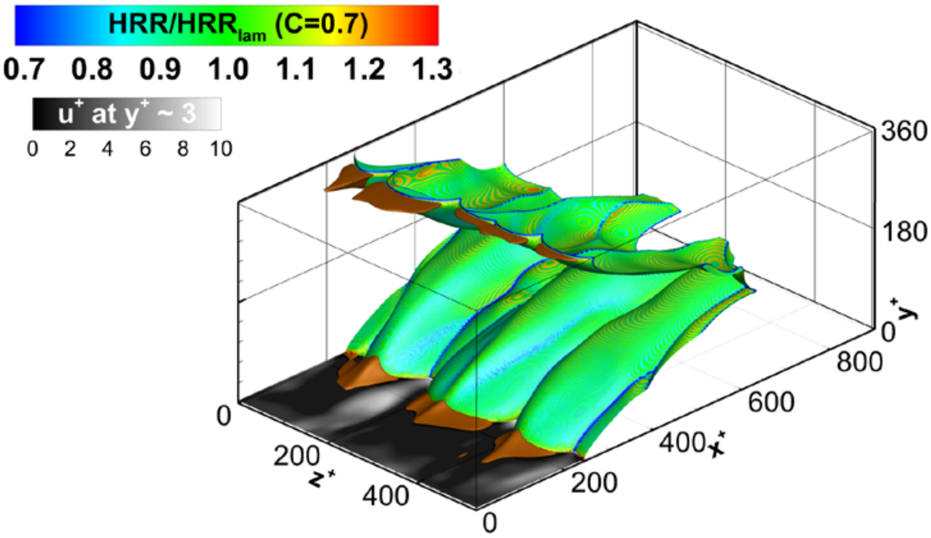

Figure 1. DNS of premixed rich hydrogen-air flame flashback in turbulent channel flow [1]. Progress variable isosurface (C = 0.7) is colored with heat release rate (HRR) scaled by HRR of the planar flame front. Scaled streamwise velocity in the y+ = 3 plane is shown by grey. Backflow regions are shown by the brown isosurface.

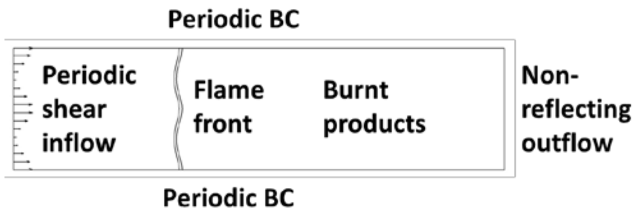

Figure 2. Sketch of the numerical setup.

instability-induced flame shape, in line with findings of Ref. [1] described above. Flame speeds for both shear flow-induced flame shape and DL-instability induced flame shape are found to be dependent on shear flow velocity fluctuation amplitude and wavelength.

2 Numerical Method

Two-dimensional computations are performed using the direct numerical simulation (DNS) compressible code S3D [8]. A planar flame configuration subjected to oncoming periodic (sinusoidal) shear flow with amplitude *A* and wavelength *L* is adopted. Figure 2 illustrates the numerical setup. An initially planar laminar stoichiometric hydrogen-air flame front is initialized from PREMIX [9] in a 2D domain, with periodic and inflow/outflow boundaries. Reactants enter from the left boundary. Periodic shear is superimposed over the mean inflow velocity, which is modified during the simulation run based on the integrated heat release rate in order to keep the flame within the computational domain. The simulations are performed for a range of parameters *A*, *L* and computational domain widths. The computational domain is 1 cm wide, with variable size in the vertical direction, employing a uniform mesh of up to 1200 x 2400 grid points. This provides a spatial resolution of 8.34e-6 m in both directions.

An explicit eighth-order central finite difference scheme for the evaluation of spatial derivatives (with fixed time step and grid spacing) [10, 11] and a fourth-order Runge-Kutta scheme for temporal derivatives are employed in S3D in the solution of the full compressible Navier-Stokes, species, and energy equations for a reacting gas mixture. The reader is referred to Ref. [8] for the detailed set of equations employed. Detailed chemical kinetics, thermodynamic and transport properties are computed with CHEMKIN [12] and TRANSPORT [13] libraries. The mechanism of Li et al. [14] involving 9 species and 19 elementary reactions is employed and transport properties are evaluated using mixture average formulae.

For all cases studied the thermodynamic pressure is held constant at 1 atm, with equivalence ratio equal to 1.0 (stoichiometric conditions), and the unburnt temperature T_0= 298K. The laminar burning velocity for these conditions is S_L = 2.07 m/s, and flame thickness is δ_T=0.397 mm. Non-reflecting outflow NSCBC is applied on the right boundary, providing no contamination of results by reflected pressure waves [15], and soft inflow boundary condition is applied on the left boundary. Translational periodic boundary conditions are prescribed at the top and bottom boundaries. For further details on the computational methodology and boundary conditions the reader is referred to Ref. [16].

3 Flame configuration swap during propagation

It was observed that flame configuration can experience modification during the simulation run. Figure 3 shows the example of how an initial shear flow-induced flame configuration can be replaced by a stable DL-instability induced configuration during the DNS run. Figure 3 (left) shows the two-cusp shear flow-induced flame shape that is subsequently replaced by one-cusp flame shape, see Fig. 3 (right). The onset of the one-cusp flame shape is associated with thermal expansion of the burnt gases and DL instability of the flame front.

Similar phenomenon was observed in Ref. [1], where it was found that boundary layer streaks determine the flame front shape initially; however, at the later stages of the boundary layer flashback the Darrieus-Landau instability starts to dominate the flame front shape, see Fig. 4. Due to the high numerical cost of 3D DNS, it would be difficult to perform the parametric study for different flow parameters. For that reason, here we perform 2D simulations to study how the flame velocity for both configurations depends on the shear flow velocity fluctuation amplitude and wavelength.

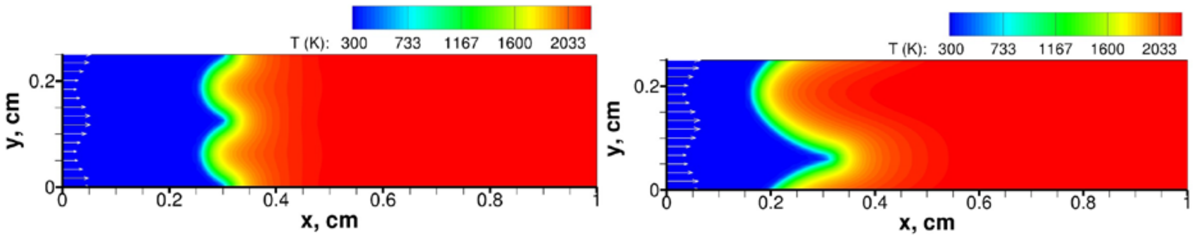

Figure 3. The dominating wavelength of the propagating flame can spontaneously change from shear-flow to DL-instability induced one. (left) t= 3 ms, (right) t=7 ms. Arrows on the left illustrate the shear flow velocity amplitude.

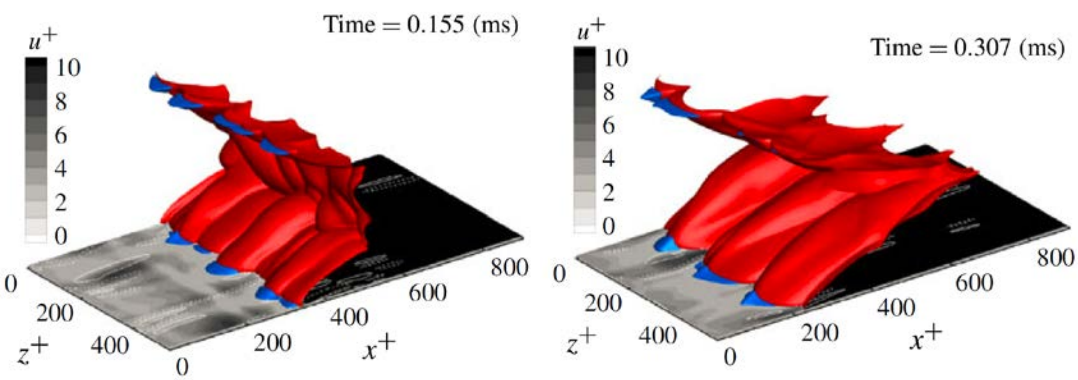

Figure 4. DNS of premixed rich hydrogen-air flame flashback in turbulent channel flow [1]. Progress variable isosurface (C = 0.7) is shown by red. Scaled streamwise velocity in the y+ = 3 plane is shown by grey. Backflow regions are shown by the blue isosurface.

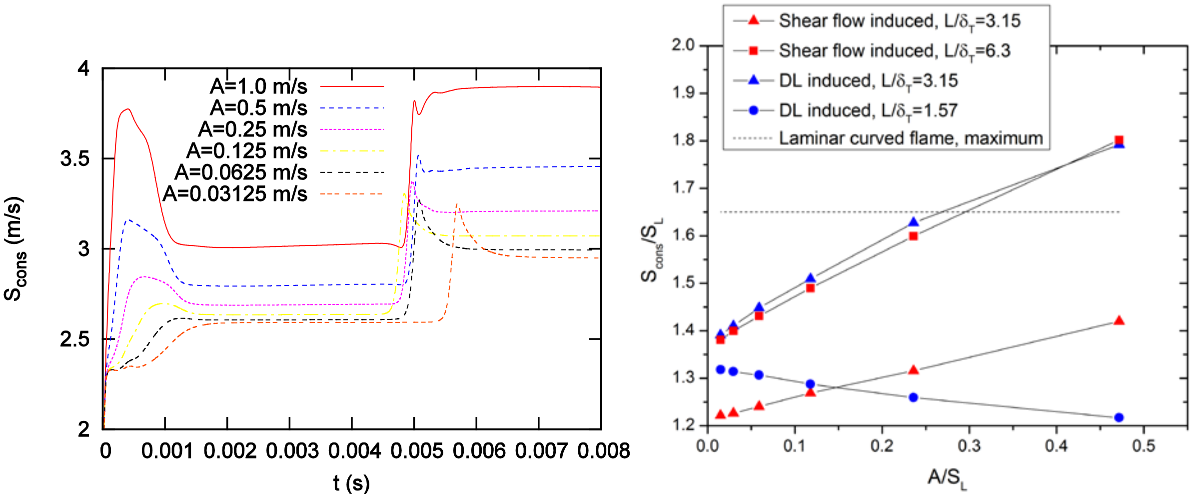

Figure 5. Left: Flame velocity evolutions for L/δ_T =6.3 and A=0.03125 – 1 m/s. DL-instability induced regime onset is observed within the time interval between 5 ms and 7 ms. Right: Shear flow and DL-instability induced stationary flame velocities versus velocity fluctuation amplitude. Dashed line shows the theoretical estimate of the maximum laminar curved flame speed, Ref. [17].

4 Dependence of flame speed on flow perturbation amplitude

Figure 5 (left) shows the flame velocity evolution for a given domain width and a range of periodic shear flow velocity fluctuation amplitudes A. We see that for each A the velocity evolution graphs show two distinctive stationary stages. The first stationary stage, spanning up to approximately 5 ms for each velocity graph, is associated with the shear-flow induced flame shape (illustrated by Fig. 3 (left)), while the second stationary stage is associated with DL-induced flame shape (see Fig. 3 (right)). It is observed that the speed of the shear flow-induced flame (i.e. the first stationary stage on Fig. 5 (left)) grows with A, in line with findings of Brailovsky and Sivashinsky [5] for the flames with zero thermal expansion.

Figure 5 (right) shows both shear-flow induced (first stage) and DL-instability induced stationary flame (second stage) velocities versus scaled shear flow perturbation amplitude A/S_L. It is seen that DL-induced flame speed grows with A in sufficiently wide domains, however, in narrow domains the inflow may mitigate the transition to the second DL-dominated configuration.

In Ref. [18], the laminar curved flame theory [17] was used to analytically estimate the DL-induced flame speed. It is noted that the maximum laminar curved flame speed of Ref. [17] shown by the dashed line in Figure 5 (right) appears to be in reasonable agreement with the present results.

5 Dependence of flame speed on flow perturbation wavelength

Figure 6 shows the scaled shear-flow induced stationary flame velocities S_{cons}/S_L versus scaled shear flow velocity fluctuation wavelength L/δ_T. It is observed that for each velocity fluctuation amplitude A the shear flow induced stationary flame velocity has non-monotonic dependence on the flow perturbation wavelength L. The velocity perturbation wavelength, at which the maximum of the stationary flame velocity is observed, may be associated with the fastest growing DL instability harmonic wavelength. For the current case, the fastest growing DL instability harmonic wavelength is approximately 14.8δ_T, as predicted by the theory of Ref. [17].

It is noted that for all velocity fluctuation amplitudes A the curves on Figure 6 show the same non-monotonous trend, with velocity maximum happening close to 14.8δ_T. On the one hand, this is an

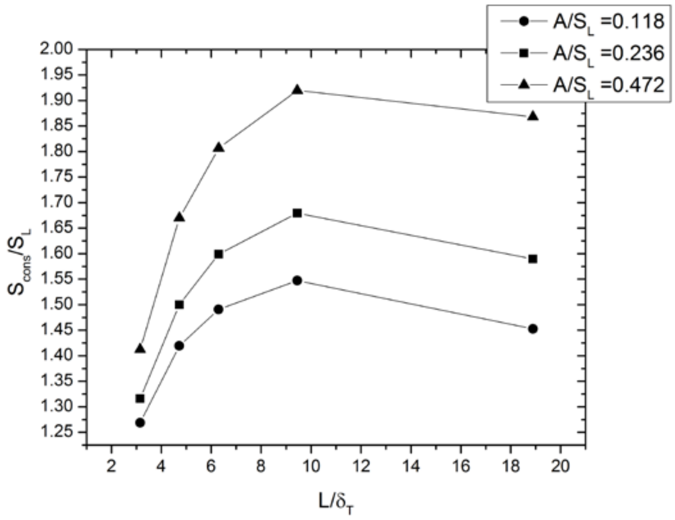

Figure 6. Shear flow induced stationary flame velocities versus shear flow perturbation wavelength.

additional indication that the flame velocity on the second stationary stage (see Fig. 3 (right)) is indeed dominated by the DL instability. On the other hand, it is clear that the higher is the oncoming shear flow velocity amplitude *A*, the higher is the final maximum flame velocity on the second DL instability-dominated stage. Based on this observation, it is possible to conclude that the resulting flame velocity is dependent both on the thermal expansion coefficient and the oncoming shear flow parameters. To study the influence of the thermal expansion on the flame speed at both stages in further detail, an additional parametric study is needed.

6 Conclusions and future work

The present parametric study is focused on the variation of the flame propagation speed dependent upon the amplitude and spatial scale of the oncoming periodic shear flow. The study was performed through DNS of the initially planar flame in 2D domain interacting with the oncoming shear.

It is found that the initial shear flow-induced flame shape may be unstable, subsequently replaced by the DL-instability dominated flame shape, in line with findings of Ref. [1], where similar phenomenon was observed in 3D DNS of the premixed flame flashback in turbulent channel flow. Both shear flow-induced and DL instability-induced flame speeds depend on flow perturbation amplitude and wavelength. The findings are relevant to the problem of the boundary layer flashback and can potentially provide a useful guidance for developing the flashback velocity models.

Future work will include a parametric study of the dependence of stationary flame velocity on the thermal expansion ratio. Also, the DL instability-dominated flame shape onset will be studied in greater detail.

References

[1] A. Gruber, J. H. Chen, D. Valiev, C. K. Law, Journal of Fluid Mechanics 709 (2012) 516-542.

[2] C. Heeger, R. L. Gordon, M. J. Tummers, T. Sattelmayer, A. Dreizler, Exp. Fluids 49 (2010) 853-863.

[3] C. Eichler, T. Sattelmayer, ASME J. Engng Gas Turbines Power 133 (2011) 011503.

[4] D. Ebi, N. T. Clemens, AIAA paper 2013-2604 (2013) DOI:10.2514/6.2013-2604.

[5] I. Brailovsky, G. Sivashinsky, Physical Review E 51(2) (1995) 1172-1183.

[6] F. Creta, N. Fogla, M. Matalon, Combustion Theory and Modelling 15 (2) (2011) 267-298.

[7] F. Creta, M. Matalon, Journal of Fluid Mechanics, 680(1) (2011) 225–264.

[8] J. H. Chen et al., Comp. Sci. Disc., 2 (2009) 015001

[9] R. J. Kee, J. F. Grcar, M. D. Smooke, J. A. Miller, E. Meeks, PREMIX: A fortran program for modeling steady, laminar, one-dimensional premixed flames, Tech. Rep. SAND85-8240, Sandia National Laboratories (1985).

[10] C. A. Kennedy, M. H. Carpenter, Applied Numerical Mathematics 14 (4) (1994) 397-433.

[11] C. A. Kennedy, M. H. Carpenter, R. M. Lewis, Applied Numerical Mathematics 35 (3) (2000) 177-219.

[12] R. J. Kee, F. M. Rupley, J. A. Miller, Chemkin-II: A FORTRAN chemical kinetics package for the analysis of gas-phase chemical kinetics, Tech. Rep. SAND89-8009B, Sandia National Laboratories (1991).

[13] R. J. Kee, G. Dixon-Lewis, J. Warnatz, M. E. Coltrin, J. A., Miller, A fortran computer code package for the evaluation of gas-phase multicomponent transport properties, Tech. Rep. SAND86-8246, Sandia National Laboratories (1986).

[14] J. Li, Z. Zhao, A. Kazakov, F. Dryer, International Journal of Chemical Kinetics 36 (2004) 566-575.

[15] C. S. Yoo, H. G. Im, Combustion Theory and Modelling 11 (2007) 259-286.

[16] C. S. Yoo, J. H. Chen, J. H. Frank, Combustion and Flame 156 (2009) 140-151.

[17] V. Bychkov, M. Liberman, Physics Reports 325(4) (2000) 115-237.

[18] A. Gruber, A. R. Kerstein, D. Valiev, H. Kolla, J. H. Chen, Proceedings Combustion Institute 35 (2) (2015) 1485-1492.